Learning Fuzzy Control Parameters for Kite-based Tethered Flying Robot using Human Operation Data

Learning Fuzzy Control Parameters for Kite-based Tethered Flying Robot using Human Operation Data

Chiaki Todoroki and Yasutake Takahashi
Dept. of Human & Artificial Intelligent Systems,
Graduate School of Engineering, University of Fukui
3-9-1, Bunkyo, Fukui, Fukui, 910-8507, Japan
Email: {ctodoroki,yasutake}@ir.his.u-fukui.ac.jp

Takayuki Nakamura
Department of Computer and Communication Sciences,
Faculty of Systems Engineering, Wakayama University
Sakaetani 930, Wakayama 640-8510, Japan
Email: ntakayuk@sys.wakayama-u.ac.jp

***Abstract*—This research aims at realizing a flying observation system which complements other information gathering systems using a balloon or an air vehicle. We have proposed the kite-based tethered flying robot with long-term activity capability[1].**

This paper shows a computational model of the kite-based tethered flying robot and a method of learning fuzzy control parameters for the robot using human operation data.

I. Introduction

Autonomous observation systems using a balloon[2], [3] or an airplane[4], [5], [6] have been studied as a solution of information gathering systems from the sky. The balloon system is noiseless and able to stay in the sky for a long time. However, the helium gas reservation is necessary and it needs relatively long time and specialists of gas maintenance for the flight preparations. On the other hand, an airplane system needs less time for flight preparations, but a long-term activity is difficult due to limitation of the fuel.

We have proposed a tethered flying robot based on a kite that flies with wind power as one of the natural power sources and conducted some experiments with a real robot we designed and built[7]. However, wind situation often varies in real robot experiment and rain or, too strong or too weak wind situation make the real robot experiment hard. It is also difficult to evaluate the developed flight controller in various wind situation with real data. Therefore, we develop a computational simulator of the dynamics of the kite-based tethered flying robot for development of the controller that works in various wind situation. Conventional work has modeled a kite or a paraglider (for example, [8]). However, our kite-based tethered flying robot has a considerable weight attached to the flight unit and there is no paper describing the model to the best of our knowledge.

We also proposed a flight control systems based on fuzzy controllers inspired by how a human flies a kite and showed its validity in the real robot[7]. The fuzzy rule table was designed with human designer inspiration, however, it is hard to ensure that the table is correct in various wind situations. It becomes hard to define the table if the number of state variables or membership functions is big. A certain learning approach is necessary for the development of the fuzzy rule table.

This paper gives two contributions. First, we shows a computational model of the kite-based tethered flying robot taking the mass of the flight unit into consideration. A real robot experiment shows the validity of the computational model. Second, we propose a method of learning fuzzy control parameters for the robot using human operation data and shows its validity with computational simulations.

II. Kite-based Tethered Flying Robot

Our tethered flying robot consists of a kite, a flight unit, tether line, and a ground control unit. The concept of the kite-based tethered flying robot is shown in Fig.1. The flight unit carries sensors and transmits the surrounding wind state, position and orientation of the flight unit itself to the ground wirelessly. The flight unit is lifted from the ground by a kite. The ground control unit controls the line attached to the flight unit according to the data sent by the flight unit. A ZigBee module is used for wireless communication between the flight unit and the ground control unit. More details of the real robot is described in [1], [7].

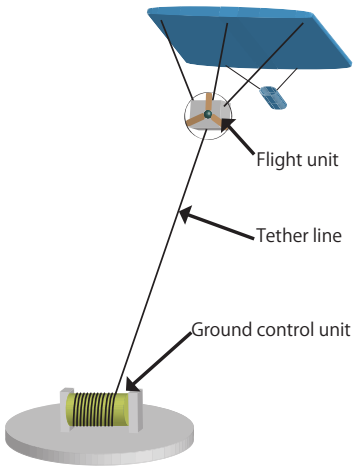

Fig. 1. Concept of kite-based tethered flying robot

A. Computational Model

Figure 2 shows the 2D model of our kite-based tethered flying robot. A kite might change its shape according to the wind situation around the kite. We assume that the kite does not change the shape too much during the flight because the

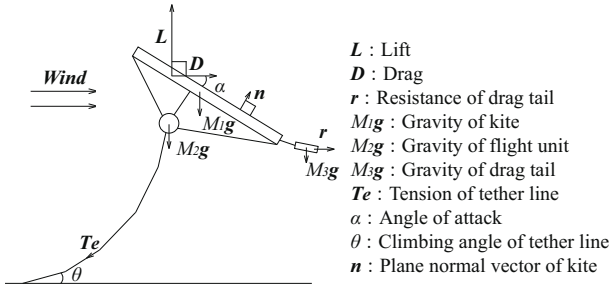

Fig. 2. Computational model of kite-based tethered flying robot

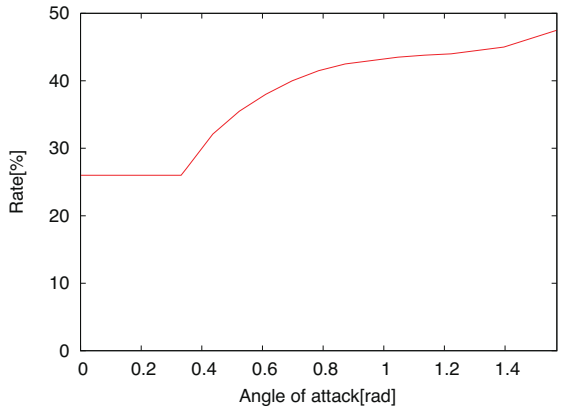

Fig. 3. Position of the point of forces to the chord length from the leading edge of the chord line

wind power is strong enough to bring the kite itself during the flight and the wind power keeps the shape of the kite. Therefore, the kite is modeled as a board in the dynamics engine simulator. We use Open Dynamics Engine (ODE)[9] for our dynamics simulator of the kite-based tethered flying robot. Lift force $\boldsymbol{L}$, drag force$\boldsymbol{D}$, and the point of the forces are modeled by reference to Okamoto et. al.[10]. Figure 3 shows the point of the forces, $\boldsymbol{L}$ and $\boldsymbol{D}$, from the leading edge of the kite. The point is ratio against the chord length. $\boldsymbol{L}$ and $\boldsymbol{D}$ are calculated with Eqs.(1) and (2).

$$\boldsymbol{L} = \frac{1}{2} C_l \rho S (\boldsymbol{U} \times \boldsymbol{n}) \times \boldsymbol{U} \tag{1}$$

$$\boldsymbol{D} = \frac{1}{2} C_d \rho S \|\boldsymbol{U}\| \boldsymbol{U} \tag{2}$$

$$\rho = \frac{1.293 P}{1.0 + \frac{t}{273.15}} \tag{3}$$

ρ is air density [$\mathrm{kg/m^3}$] and calculated by Eq.(3). P and t are atmospheric pressure [atm] and temperature [degree of centigrade], respectively. $\boldsymbol{U}$, $\boldsymbol{n}$, and S are relative wind velocity against the kite[m/s], normal vector of the kite plane, and frontal projected area[$\mathrm{m^2}$], respectively. C_l and C_d are lift and drag coefficients.

C_l and C_d are depends on the attacking angle α and the kite wing configuration. In practice, the parameters should be identified by a real wind-tunnel test, however, it is hard to conduct the wind-tunnel test with a kite. Therefore, we use Eqs.(4) and (5) according to [11]. Unfortunately, the equations offer the parameter values only when the attacking angle α is from 0 [rad] to $\frac{\pi}{4}$ [rad]. The lift coefficient C_l is therefore linearly interpolated while attacking angle $\alpha > \frac{\pi}{4}$ under constraint that $C_l = 0$ when $\alpha = \frac{\pi}{2}$. We assume that the drag coefficient C_d does not change a lot if the attacking angle α is larger than $\frac{\pi}{4}$ [rad] so that C_d when $\alpha > \frac{\pi}{4}$ is the value of C_d when $\alpha = \frac{\pi}{4}$. Those assumptions follow the work of Okamoto et. al.[10].

$$C_l = \frac{2.0 \alpha \pi}{1.0 + \frac{2.0\alpha}{A_r}} \tag{4}$$

$$C_d = 1.28 \sin \alpha + \frac{C_l^2}{0.7 \pi A_r} \tag{5}$$

where A_r is the aspect ratio of the kite wing.

The drag force of the drag tail of the kite is measured through real experiments with the drag tail of the kite and modeled to use it in a simulation. Figure 4 shows the

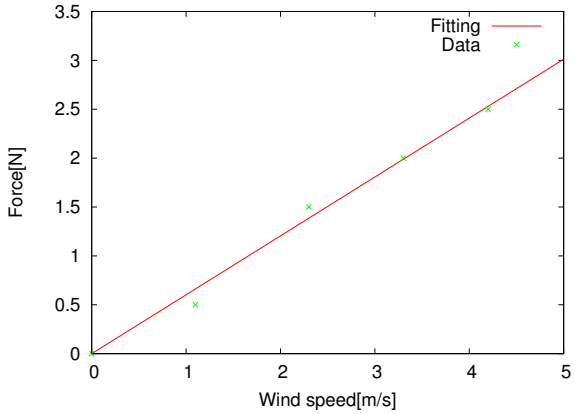

Fig. 4. Experimental result of relationship between wind speed and drag force using real drag tail of the kite

experimental result of the relationship between the wind speed and drag force using the real drag tail of the kite. From the experimental results, the drag force r of the drag tail can be estimated with a simple linear equation as below:

$$r = 0.602341 v \tag{6}$$

where v is the wind speed.

The tether line is modeled with a set of small pieces of rigid sticks because the ODE does not have a flexible line model. The line is composed with 20 small rigid stick-type bodies in this paper. Each rigid stick-type body takes gravity into account. The line-winding behavior of the ground unit is modeled as dragging the tail of the tether line. The ODE itself does not take the air friction into consideration. The real kite-based tethered flying robot has the influence of the air friction. Therefore, air viscous friction is added to each rigid body on the ODE in the direction opposite to the object relative velocity to the air. In the real experiments, a safety line is attached to the flight unit in order to avoid releasing the flight unit just in case the main tether line is cut off. The simulator

takes it into consideration, that is, the gravity force and wind viscous friction are added to the dynamics simulation. The actual flying robot catches the wind from the side, but, the computer simulator does not take it into consideration.

B. Comparison between data from Model and Real Robot

We compare the take-off flight data from the computer simulated model and the real robot. The experiment is conducted in the situation of 1.5 [m/s] wind speed on the ground. The winding machine controls the tether winding power. The real ground unit controls the power with duty ratio of the PWM module inputs to the winding motor. The simulated one controls the power with the drag force of the tether line, directly. The winding power increases from 0 to maximum in the first 3 [s], keeps the power in 15 [s], and decreases to 0 within 3 [s]. Figures 5 and 6 show the take-off behavior of the kite-based tethered flying robot under a windless situation. Figures 5 and 6 show the real robot experiment and simulated one, respectively. Figure 7 shows the motor input, winding power, length of the tether line between the winding machine and the flight unit, and wind speed against the flight unit. Figure 8 shows the altitude of the flight unit. The red and green line indicate the ones of real robot and simulated one. The data of the real robot includes sensor noises and the resolution is not high because of the altitude sensor ability, unfortunately. Even so, the behavior of the simulated flight unit during the flight is similar to the real one so that the simulator can be used for the evaluation of the performance of the flight controller.

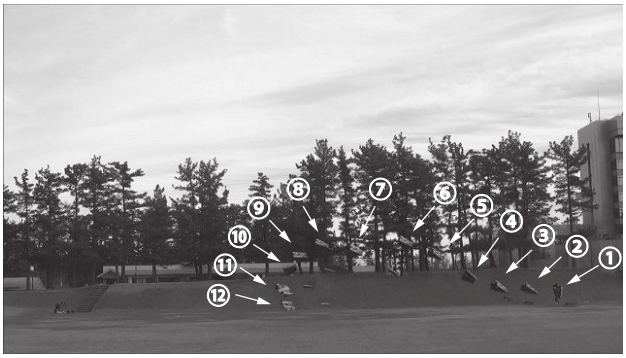

Fig. 5. Taking-off experiment result of the kite-based flying robot under a windless situation

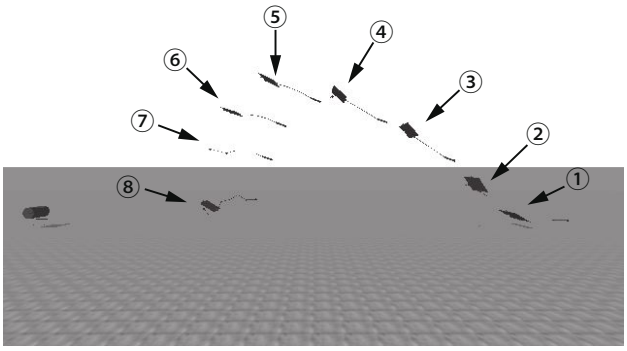

Fig. 6. Taking-off result of the computational simulated kite-based flying robot under a windless situation

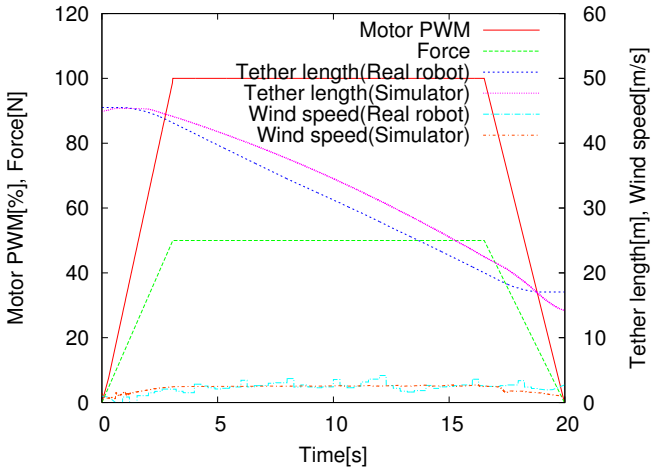

Fig. 7. Control, Teteher length, Wind speeds

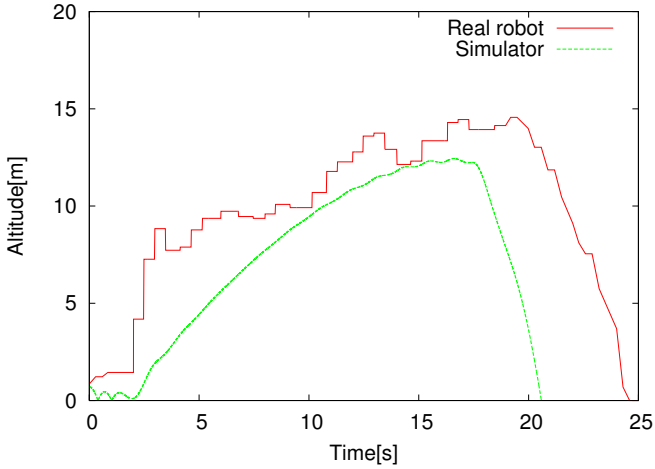

Fig. 8. Comparison of altitude

III. Fuzzy Controller for Flying

Our fuzzy controller is inspired by how a human flies a kite. Fuzzy set can reasonably represent unwritten strategy for flying a kite by human. We consider that wind speed and altitude are essential to reflect human operating characteristics. Moreover, it is necessary to take motion of the kite into account. Here, we design 3 inputs 1 output fuzzy controller for the flight. It controls the drag and release force based on a fuzzy set of altitude, altitude change of the kite and wind speed measured by the flight unit. The fuzzy controller is represented based on a simplified reasoning method by Eqs.(7) and (8).

$$\text{Rule } i : \text{if } w \text{ is } WS_i \text{ and } a \text{ is } ALT_i \text{ and } da \text{ is } DALT_i \text{ then } \varphi \text{ is } b_i \ (i = 1, 2, ..., \text{n})$$

$$h_i = \min(\mu_{WS_i}(w), \mu_{ALT_i}(a), \mu_{DALT_i}(v_a)) \quad (7)$$

$$\varphi = \frac{\sum_{i=1}^{n} h_i b_i}{\sum_{i=1}^{n} h_i} \quad (8)$$

h_i in Eq.(7) indicates the degree of rule i if the wind speed w, the altitude a, and the altitude change v_a are

given. $\mu_{WS_i}(w)$, $\mu_{ALT_i}(a)$, and $\mu_{DALT_i}(v_a)$ are membership functions corresponding to wind speed, altitude, and altitude change for the rule i, respectively. The membership functions are shown in Fig.9. Each label (WZO, WPS, and so on) corresponds to the Table I.

φ in Eq.(8) indicates control input given to the winding machine. It is calculated as the weighted sum of the output variable b_i of the rule i with the weight of h_i. $\varphi = 100$ indicates 100 [%] drag force. On the other hand, $\varphi = -100$ indicates the brake force is zero to release the tether line. $\varphi = 0$ indicates the drag force is zero and the brake force is maximum to fix the tether line length.

Table I shows the rule table of the fuzzy controller based on 3 inputs, that is, wind speed, altitude, and change of altitude. Fixed numbers in the table are b_i. If the kite falls down, the controller tends to drag the line to keep the altitude of the kite as higher as possible. If the kite goes higher, the controller reduces dragging force and releases the line if possible.

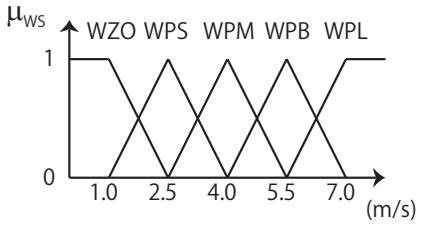

(a) Wind speed

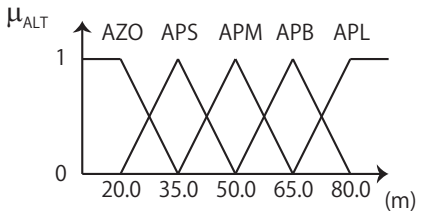

(b) Altitude

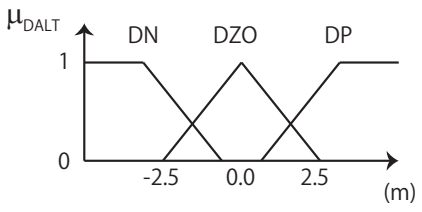

(c) Altitude change

Fig. 9. Antecedent membership function

IV. Fuzzy control parameter learning using human operation data

It tends to become hard to define the rules correctly if the number of inputs or membership functions for the fuzzy rule table becomes large. It is worth to introduce a learning method for the development of the fuzzy rule table. As the fuzzy controller is inspired by how a human flies a kite, the learning of the parameters is also based on the human operation data.

TABLE I
Fuzzy rule table

				Altitude				
				AZO	APS	APM	APB	APL
Wind speed	WZO	Altitude change	DN	100	100	100	100	100
			DZO	100	100	70	30	0
			DP	100	70	30	0	0
	WPS	Altitude change	DN	70	70	70	30	30
			DZO	30	0	0	0	0
			DP	0	0	0	0	0
	WPM	Altitude change	DN	70	70	30	30	30
			DZO	30	0	-30	0	0
			DP	0	-30	-30	0	0
	WPB	Altitude change	DN	70	30	30	30	30
			DZO	-30	-30	-30	0	0
			DP	-70	-70	-70	0	0
	WPL	Altitude change	DN	30	30	30	30	0
			DZO	-70	-70	-70	0	0
			DP	-100	-70	-70	0	0

The human operation data are collected on the computational simulator developed in the previous section while a human operates with the simulated kite-based tethered flying robot.

The wind in the simulator is generated by sine function with wind speed range from 0.0 to 4.0 [m/s] and 20 [s] cyclic period. The line length between the winding machine and the flight unit is set 50 [m] and the flight unit is on the ground when the data collection experiment starts. The human operates the motor inputs, the duty ratio of PWM, of the winding machine for 300 [s]. Figure 10 shows the collected data. The red, green, blue, purple, and cyan lines indicate altitude of the flight unit, human-operated motor input to the winding machine, length of the tether line between the winding machine and the flight unit, relative wind speed against the flight unit, and the wind speed on the ground, respectively. The human operation data are collected every 0.2 [s] for 300 [s] so that the data size is 1500 in total.

The output variable b_i in the fuzzy rule table is updated with the human operation data. Eq.(9) shows the learning equation which we refer learning method based on simplified fuzzy inference model proposed by Ichihashi et. al.[12].

$$b_i \leftarrow b_i + \beta h_i \delta \tag{9}$$

where β is learning rate. $\beta = 0.1$ in this paper. δ is the difference between the output from the fuzzy controller φ and the output of the human operation data φ^* as $\delta = \varphi^* - \varphi$.

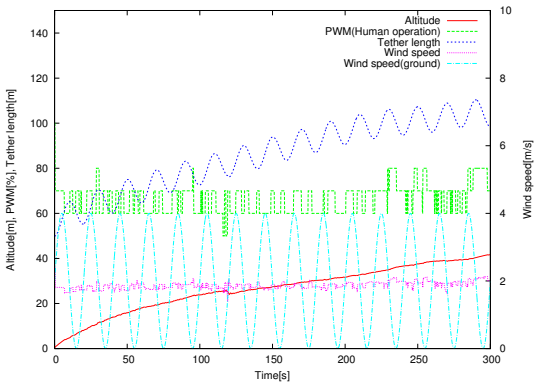

Fig. 10. Flight log with human operation on the simulator

A. *Simulation based on Learned Fuzzy Rule Table*

Figure 11 shows the flight logs before and after the learning. The initial tether line length between the winding machine and the flight unit is set to 50 [m]. Each number in the figures indicates the sequence of the position of the flight unit. Figure 12 shows the comparison of altitude of the flight unit during the flight before/after the learning. The red, green, and blue lines indicate the log using the original fuzzy rule table, the log based on human operation, and the log using the learned fuzzy rule table, respectively. The learned fuzzy controller flies the kite more rapidly than the original fuzzy controller and the human operation. It learns the fuzzy rule well from the human operation data so that it works from the start to about 100 [s].

Unfortunately, the altitude of the flight unit goes down suddenly around 120 [s]. Figure 13 shows the flight log after the learning. The red, green, blue, purple, and cyan lines indicate altitude of the flight unit, motor input to the winding machine, length of the tether line between the winding machine and the flight unit, relative wind speed against the flight unit, and the wind speed on the ground, respectively. The reason of the drop in altitude is that the controller tends to drag the line when the elevation angle between the ground and the flight unit becomes high. In case that the elevation angle is low, the flight unit tends to gain the altitude if the system drags the tether line. However, in case that the elevation angle is high, for example, it is about right angle, the flight unit tends to lose the altitude if the winding machine drags the tether line. If the length of the tether line between the winding machine and the flight unit becomes short, the elevation angle becomes smaller, then, the dragging the tether line leads the flight unit to gain the altitude, again, as Fig.13 shows, for example, from 130 to 180 [s]. Eventually, the flight unit repeats up and down, and touches down at about 330 [s].

Next, we conduct another simulation under the condition that the initial length of the tether line between the winding machine and the flight unit is set to 100 [m]. Figure 14 shows the altitude log comparison during the flight. The red and green lines indicate the logs before and after learning, respectively. The log after the learning shows that the flight unit goes high altitude in short time. However, it shows that the flight

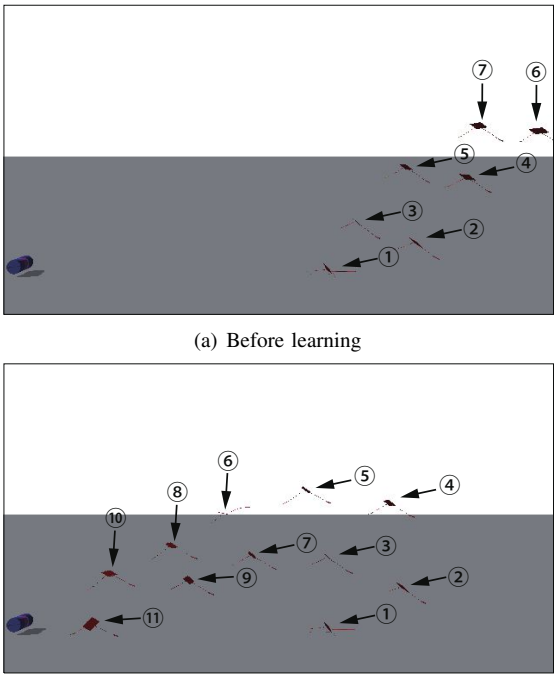

(a) Before learning

(b) After learning

Fig. 11. Flight log in simulations before/after learning

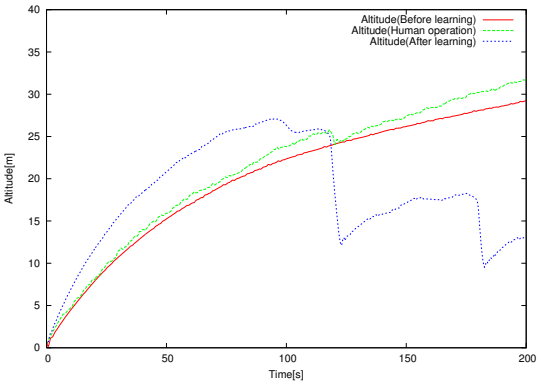

Fig. 12. Altitude comparison during the flight: Initial length of tether line between the winding machine and the flight unit is 50 [m].

unit goes down slowly after it reaches the highest position, unfortunately, again.

Figure 15 shows the flight log. It shows the length of the tether line is becoming short but the flight unit does not lose the altitude so much comparing to Fig.13. However, this result suggest that the length of the tether line becomes short, the elevation angle becomes high, then, the sudden drops of the flight unit might occur in the long flight.

The computer simulation shows the learned fuzzy controller realizes the faster and more efficient take-off behavior the human operation, however, it causes sudden drops in a long flight. The performance of the human operation is similar to one of the the initial fuzzy controller and it does not show the sudden drop in the long flight. Actually, the human operator controls the flight unit as the elevation angle between the

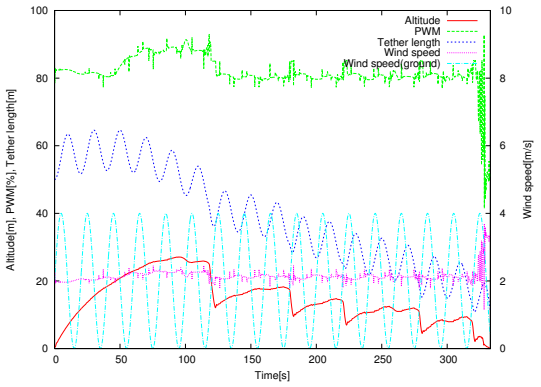

Fig. 13. Flight log after learning: Initial length of tether line between the winding machine and the flight unit is 50 [m].

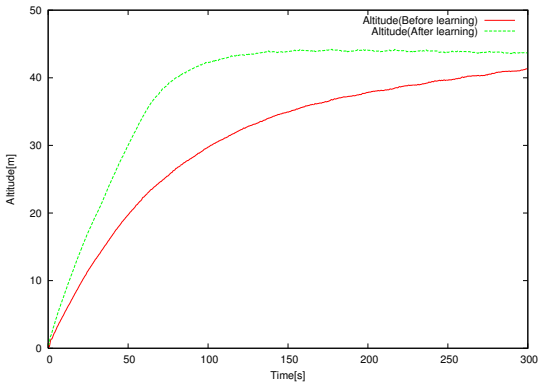

Fig. 14. Altitude comparison during the flight: Initial length of tether line between the winding machine and the flight unit is 100 [m].

ground and the flight unit does not become too high. The human operator might use the elevation angle information for the controlling the kite-based tethered flying robot.

V. Conclusion and Future Work

This paper presented a computational model of the kite-based tethered flying robot taking the mass of the flight unit into consideration. A real robot experiment showed the validity of the computational model. The paper also proposed a method of learning fuzzy control parameters for the robot using human operation data and showed its validity with computational simulations. The simulation suggests that the learning works well especially for take-off behavior. It also suggests that the additional information is necessary for more stable behavior acquisition for a long-term flight.

One of future work is to extend the fuzzy controller from 3 inputs 1 output system to 4 inputs 1 output system in order to realize more stable control for the long-term flight. Reinforcement learning is interesting to be apply for this task although this paper proposed to use a supervised learning with human operation data. Real robot experiments are also one of the future work.

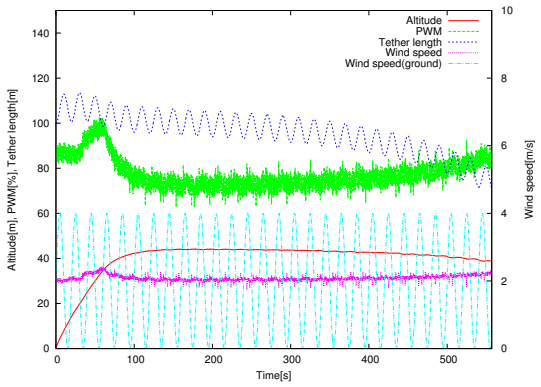

Fig. 15. Flight log after learning: Initial length of tether line between the winding machine and the flight unit is 100 [m].

ACKNOWLEDGMENT

This work was partially supported by JSPS KAKENHI Grant Number 24650118.

References

[1] T. Ishii, Y. Takahashi, Y. Maeda, and T. Nakamura, "Tethered flying robot for information gathering system," in *IROS'13 Workshop on Robots and Sensors integration in future rescue INformation system (ROSIN'13)*, November, 2013.

[2] H. Aichi, M. Kumada, T. Kobayashi, Y. Sugiyama, K. Horii, and S. Yokoi, "Application to power generation by wind and environmental watching and/or it system by floating platform tethered with cable, and preliminary study on climbing characteristics of a tethered aerodynamic platform with side-by-side twin rotors," *Bulletin of Daido Institute of Technology*, vol. 38, pp. 213–223, 2002.

[3] ——, "Application of floating platform tethered with cable in high altitude to wind power generation, telecommnication / broadcasting, and environmental watching," *Denkiseiko*, vol. 74, no. 3, pp. 167–172, 2003.

[4] S. Karim and C. Heinze, "Experiences with the design and implementation of an agent-based autonomous uav controller," in *Proceedings of the fourth international joint conference on Autonomous agents and multiagent systems*. New York, NY, USA: ACM, 2005, pp. 19–26.

[5] J. Fujinaga, H. Tokutake, and S. Sunada, "Guidance and control of a small unmanned aerial vehicle and autonomous flight experiments," *Journal of the Japan Society for Aeronautical and Space Sciences*, vol. 56, no. 649, pp. 57–64, 2008-02-05. [Online]. Available: http://ci.nii.ac.jp/naid/10021152872/

[6] T. Suzuki, J. Meguro, Y. Amano, T. Hashizume, D. Kubo, T. Tsuchiya, S. Suzuki, R. Hirose, K. Tatsumi, K. Sato, and J. Takiguchi, "Development of information collecting system using a small unmanned aerial vehicle for disaster prevention and mitigation," *Journal of Robotics Society of Japan*, vol. 26, no. 6, pp. 553–560, 2008-08-29. [Online]. Available: http://ci.nii.ac.jp/naid/10024269382/

[7] T. Ishii, Y. Takahashi, Y. Maeda, and T. Nakamura, "Fuzzy control for kite-based tethered flying robot," in *Proceedings of 2014 IEEE World Congress on Computational Intelligence*, vol. DVD-ROM, July 2014, pp. 746–751.

[8] M. Canale, L. Fagiano, and M. Milanese, "High altitude wind energy generation using controlled power kites," *IEEE Control Systems Society*, vol. 18, pp. 279–293, March.2010.

[9] R. Smith, "Open dynamics engine," 2008, http://www.ode.org/. [Online]. Available: http://www.ode.org/

[10] T. Okamoto, M. Fujisawa, and K. T. Miura, "Development of a user inteactive kite simulation system (in japanese)," in *Graphics and CAD / Visual Computing Joint Symposium 2009*, June 25-26, 2009.

[11] "Nasa kite modeler 1.5a," http://www.grc.nasa.gov/WWW/K-12/airplane/kiteprog.html, 2013/11/07.

[12] H. Ichihashi and T. Watanabe, "Learning control by fuzzy models using a simplified fuzzy reasoning," *Japan Society for Fuzzy Theory and Systems*, vol. 2, no. 3, pp. 429–437, August 15, 1990.